TRENDS IN THE *F*2-LAYER PARAMETERS BASED ON THE SVERDLOVSK (ARTI, 56 N) STATION DATA

A. D. Danilov[a,*], A. V. Konstantinova[a], I. A. Ryabukhin[b]

[a]*Fedorov Institute of Applied Geophysics, Moscow, Russia*

[b]*Bulashevich Institute of Geophysics, Hermann & Robert Abels laboratory-observatory «Arti», Arti, Sverdlovsk oblast, Russia*

**e-mail: adanilov99@mail.ru*

Received December 05, 2024

Revised January 27, 2025

Accepted April 14, 2025

Abstract. Long-term variations (trends) in two parameters of the ionospheric *F*2 layer (*foF*2 and *hmF*2) based on the observations at the Sverdlovsk (Arti) ionospheric station and the calculated values of TEC over that station are analyzed. Five near-noon moments of LT are considered. Principal analysis is performed for three winter months, but for the sake of comparison, the values of the trends in *foF*2 and *hmF*2 for the spring month April, summer month July and fall month October are also presented. A confirmation of the existence of seasonal variations in the *foF*2 trends is obtained: negative trends are the strongest in winter. The obtained results agree with the results obtained earlier for midlatitude stations of the Northern and Southern hemispheres. No substantial seasonal variations are found for the *hmF*2 trends. Trends in the TEC values over the aforementioned station are also considered. It is demonstrated that there is a reasonable agreement between the relative trends (in percent) in *foF*2 и TEC.

Keywords: *long-term trends, ionospheric F2 layer, diurnal variations*

DOI: 10.31857/S00167940250407e6

1. INTRODUCTION

The problem of long-term changes in the upper atmosphere parameters is well known and actively discussed in the literature. A detailed consideration of this problem and a description of the results of recent studies can be found in the reviews by Laštovička [2023] and Cnossen et al. [2024]. Special attention is paid to the analysis of long-term changes (trends) of the ionospheric *F2* layer parameters.

The study of the problem of ionospheric trends has become noticeably more intensive in recent years. This concerns both the "classical" parameters *foF2* and *hmF2* and such parameters as the total electron content TEC and the *F2* (slab thickness) ST. A brief review of recent publications can be found in Danilov and Berbeneva [2025]

Analysis of the results of vertical sounding (VS) of the ionosphere at the stations of the global VS network is the most frequently used method of searching for trends of the *F2* layer parameters. Without diverting to the discussion of all approaches and results and referring the reader to the above reviews, we note only that data from different VZ stations scattered around the globe are considered. Data from some stations (e.g., Juliusruh, Rome, Townsville) have been analyzed several times by different groups of authors. The key issue is, of course, the presence of a homogeneous data series for a long (several solar activity cycles) period of time.

In this paper, we analyze the results of *foF2* measurements at Sverdlovsk (Arti) station (56°26' N, 58°34' E). To the best of our knowledge, these data have not yet been used to search for long-term trends. For completeness of the picture, the data of the total TEC electron content for the position of the indicated station are also considered

A large series of studies of trends in the *F2* layer parameters (*foF2* and *hmF2*) has been performed during the last decade at the Institute of Applied Geophysics. We will compare the results obtained below with the results of the recent work by Danilov et al. [2024a], which analyzes in detail the *foF2* trends from data of six stations of the Northern and Southern Hemispheres.

Previously, a method for determining the long-term trends of the ionospheric *F2* layer parameters was developed and repeatedly used. A rather detailed description of the method can be found in Danilov and Berbeneva [2023]. Here we will remind only that the method is based on comparison of *foF2* values during the last two decades with *foF2* values for the same conditions during the "reference" period 1957-1980, when there were no anthropogenic *foF2* trends yet. Between the corresponding *foF2* values the difference Δ *foF2* is calculated, change of which with time during the analyzed period 1996-2024 gives the desired trend *k*(*foF2*).

When determining the trends of ionospheric parameters, the question of the choice of solar activity (SA) indices to eliminate the SA effects is very important. The question was discussed by many researchers. Let us note here only two works of the Argentine group [De Haro Barbás and Elias, 2020; De Haro Barbás et al., 2021] and the publications of Laštovička [2024] and Laštovička and Burešová [2023]. Recent works of the mentioned group [Zossi et al., 2024; 2025] consider the selection of the best CA trend precisely in terms of the resulting *foF2* trends.

In [Danilov and Berbeneva, 2024; Danilov et al., 2023a; Danilov and Berbeneva, 2023], the question of the quality of description of the change in *foF2* with time by different CA indices was considered in detail. The conclusion of these works is that the best description is provided by the F30 index, followed by the Ly-α and *MgII* indices. The worst for this description is the *Rz* (sunspot number) index. Following these results, in this paper we used the *F30*, Ly-α , and *MgII* indices to eliminate the CA effects.

It is known (see Danilov and Konstantinova [2015], Yue et al. [2018], Duran et al. [2023]) that the *foF2* trends show a pronounced diurnal course - the values of *k*(*foF2*) are negative and significant in amplitude during the day and small at night. That is why in this paper we analyzed the trends for all months for five midday hours of local time: 10:00, 11:00, 12:00, 13:00, and 14:00 LT.

The greatest attention was paid to the winter months, since it is for them that the most well-defined trends are observed [Danilov et al., 2024a; Duran et al., 2023]. However, to further verify the seasonal variations of *foF2* trends, we also performed the corresponding calculations for April, July, and October.

2. RESULTS

2.1 foF2 trends for winter months

As mentioned above, we analyzed *foF2* measurements by the VZ method at Sverdlovsk station at around midday hours of three winter months. For January and February, data up to 2024 were available. For December, data for 2023 were missing for technical reasons, so the analyzed data series ended in 2022

Examples of variations with time of the values Δ *foF2*, the slope of the linear approximation of which gives the desired value *k*(*foF2*), for winter months using different CA indices are shown in Figs. 1-3. In all figures in this paper, the values of *k*(*foF2*) are given in units of MHz per year. The values of the certainty coefficient R^2 by Fisher's F-test, which characterize the statistical significance of the obtained S dependencies, are also given.

Figure 1.

Figure 2.

Figure 3.

As can be seen from these figures, using all three CA indices for all three winter months, there is a well pronounced decrease in the value of Δ *foF2* with time. The R^2 values indicate the significance of the obtained dependencies. Recall that according to the Fisher's F-test with the available number of points, the R^2 values shown in the figures give a statistical significance *S* that exceeds 98%. The observed decrease of Δ *foF2* with time gives negative values of the trend *k*(*foF2*), which are not significantly different from each other.

The results for winter months are summarized in Table 1. The SD values show the RMS error when averaging the values of *k*(*foF2*) for each situation (month, CA index) over all five LT moments.

Table 1.

Table 1 shows that averaging over all five LT moments yields quite reasonable values of *k*(*foF2*) for each situation (month, CA index) with relatively small SD values.

If we consider the average over all CA indices of the *k*(*foF2*) values for each month, we obtain the following values: -0.031, -0.037 and -0.035 MHz per year for December, January and February, respectively. As we can see, the agreement between the three winter months is very good.

Comparison of the obtained mean trends for Sverdlovsk station with the results for other stations from the work of Danilov et al. [2024a] is given in the Discussion.

In some panels of Figures 1-3, the dashed line shows the trend in Δ *foF2* over the recent few years. We will return to this fact below.

The "Delta" method proposed earlier in [Danilov and Konstantinova, 2017] is the most illustrative method for determining the nature and approximate amplitude of *foF2* trends. It is based on the same comparison of *foF2* values for a given index of solar activity in the "reference" period (1957-1980), when there were no trends of anthropogenic nature, and in the analyzed period, as the main method. In the trend there are no artificial procedures (smoothing, averaging, etc.) - two curves (dependences of *foF2* on the selected CA index in each of the periods) are compared, and their difference gives the change in *foF2* (Delta value) for the time elapsed after the "reference period". A more detailed description of the Delta method and the results of analyzing the data for Juliusruh station by this method can be found in Danilov et al. [2023б].

A detailed study of the trends for many stations using the Delta method requires a separate publication. We shall limit here only to the calculation of the Delta values for the winter months using the same data of Sverdlovsk station, which are used in this work for searching the trends of *foF2* and hmF2, and comparison of the obtained values with the above-mentioned results for Juliusruh station.

We compared the dependencies of monthly median *foF2* on different CA indices in the "reference" period and two recent periods 1996-2024 and 2013-2024. Examples of this comparison for January are shown in Fig. 4. Dots are purely experimental values of median *foF2* for the respective month and LT moment, plotted as a function of the CA index for that month. The curves are approximations of these points by a 3rd degree polynomial. Intervals of years and values of certainty coefficient by Fisher's F-test are given near the curves.

Figure 4.

Figure 5.

A similar comparison for February is presented in Fig. 5.

As can be seen from the examples shown in Figs. 4 and 5, the curves of approximation of *foF2* dependence on CA index for the analyzed periods are significantly lower than for the reference period. Averaging the difference between the two curves gives the desired Delta value (denoted as *D*) for each situation (LT moment, month, CA index). The results of determining *D*(*foF2*) for winter months are given in Table 2.

Table 2.

As can be seen from this table, the same pattern is observed for all situations - the value of *D*(foF2) is negative and its magnitude is higher for the later period 2013-2024 than for the period 1996-2024. In other words, the values of *foF2* at each fixed CA level are smaller in the analyzed periods than in the reference period 1958-1980. Moreover, this decrease is stronger for the later analyzed period.

As mentioned above, this method does not give the values of the trend *k*(*foF2*). But the tendency of *foF2* values to decrease from the reference period to the analyzed period is clearly visible. This agrees with the specific values of foF2 trends obtained in this paragraph.

Danilov et al. [2023b] calculated *D*(*foF2*) values using data up to 2022 for Juliusruh station. A comparison of the results of these calculations with the results for Sverdlovsk station is given in Table 3. As can be seen from this table, the *D*(*foF2*) values averaged over the LT moments for both months and both CA indices for the two stations agree quite well with each other.

Table 3.

Without diverting to a detailed discussion of *D*(*foF2*) values and their variations, we simply note that, on average, the systematic decrease of the critical frequency of foF2 from the reference period to the recent decade is 0.8-0.9 MHz for the data of Sverdlovsk station analyzed in this work. Sverdlovsk 0.8-0.9 MHz.

2.2 Results for other seasons

We also considered data for a typical spring month of April, a typical summer month of July, and a typical fall month of October. Examples of the resulting time dependencies of the values of Δ *foF2* for April and October are shown in Fig. 6. In order not to overload the paper, we present only one example each for these months. For July, the trends are small and a strong scatter of points is observed

Figure 6.

Table 4.

The results for the three months under consideration are summarized in Table 4.

Figure 6 and Table 4 suggest the following. Better or worse negative trends are visible for all situations (LT moment, CA index, month). For the summer month of July, the negative values of *k*(*foF2*) are much smaller than for the winter months (see previous paragraph). At the same time, the scatter of the values ofΔ *foF2* relative to the approximating line is much stronger. The scatter of *k*(*foF2*) values for different LT moments but the same CA index is also stronger.

Averaging over all CA indices the *k*(*foF2*) values for July gives an average value equal to -0.013 MHz per year.

Several publications have been devoted to the analysis of seasonal variations of *foF2* trends. Without diverting here to their detailed discussion, we only note that all of them give a pronounced seasonal course: noticeable negative trends in winter months and small in amplitude (negative or positive) trends in summer. Thus, in the work of Danilov and et al. [2023b], a mean value of *k*(*foF2*) equal to -0.018 MHz per year is obtained for the summer month of June using data from St. Juliusruh. It is easy to see that the trend for Sverdlovsk station for July is close to this value.

If we average the average trends for April for each CA index, we obtain *k*(*foF2*) = -0.023 MHz per year (see Table 4). The same value for October would be -0.020 MHz per year. These values lie (as they should for the spring and fall months) between the values for winter (three-month average of *k*(*foF2*) = -0.034 MHz per year, see Table 1) and the value given in Table 4 for July (-0.013 MHz per year).

3. hmF2 TRENDS

The initial values of the M3000 coefficient were obtained by the VZ method at Sverdlovsk station (Arti). These values were recalculated to the *F2* layer height *hmF2* using the well-known Shimazaki formula. The *hmF2* values were analyzed by the same method as the *foF2* values (see above).

Examples of changes in *ΔhmF2* values for winter months and different CA indices are shown in Figs. 7-9. All trend values of *k*(*hmF2*) are given in km/year.

Figure 7.

Figure 8.

Figure 9.

Figures 7-9 show a well-defined decrease of ΔhmF2 with time. The R^2 values are in general slightly higher than for the *ΔfoF2* dependences in Figures 1-3. The observed decrease of *ΔhmF2* with time gives negative trend values of *k*(*hmF2*)

The results for the winter months are summarized in Table 5. Trends for all five LT moments are given, as well as mean values for all these moments and for all three CA indices.

Table 5.

Table 5 shows that there is reasonable agreement between the values of *k*(*hmF2*) for different LT moments within a particular situation (month, CA index). This can be clearly seen from the values of the standard deviation of SD.

The agreement of the mean values of *k*(*hmF2*) for the same month but different CA indices allows us to obtain the mean values equal to -1.21 and -0.83 km/yr for January and February, respectively. These values agree well with the results of determining *k*(*hmF2*) for Moscow station [Danilov et al., 2024b]: -0.92 and -0.64 km/yr for January and February, respectively.

To check the presence of seasonal variations of hmF2 trends, we also analyzed data for April, June, July, and October. Examples of *ΔhmF2* change with time for these months are shown in Fig. 10.

Figure 10.

To avoid overloading the paper with large tables like Tables 1 and 5, we present the results of *hmF2* trends for four months as Table 6.

Table 6.

Table 6 shows that the values of *k*(*hmF2*) averaged over the five LT moments and the three CA indices are close each other. They are only slightly smaller than the average value of -1.05 km/yr for the two winter months (see above). Averaging over the five LT moments gives in each situation (month, CA index) average values with rather low standard deviation.

Summarizing, we can note that our data analysis for Sverdlovsk station leads to the main conclusion: the F2 layer height systematically decreases at a rate of about 1 km per year. In contrast to the critical frequency trends, no pronounced seasonal variation of *k*(*hmF2*) is observed: the mean value for the two winter months is only slightly higher than the corresponding values for the summer and equinox months.

We applied the same "Delta" method to the *hmF2* data for Sverdlovsk station used above for trend extraction as to the *foF2* data (see previous paragraph)

Examples of *hmF2* changes at different time intervals are shown in Fig. 11.

The results of calculating the values of *D*(*hmF2*) are presented in Table 7, which is completely similar to Table 2.

Figure 11.

Table 7.

As can be seen from this table, the same pattern is observed for all situations - the value of *D*(hmF2) is negative and its amplitude is higher for the later period 2013-2024 than for the period 1996-2024. In other words, the height of the *F2* layer at each fixed CA level is smaller in the analyzed periods than in the reference period 1958-1980. Moreover, this decrease is stronger for the later analyzed period.

4. TEC TRENDS

We computed trends in total electron content using the following approach. We converted the TEC maps from a database that is based on JPL's GPS TEC IONEX MAP data and taken from the IZMIRAN website (see Acknowledgements).

Since the global TEC maps have a resolution of 2.5° in latitude and 5° in longitude, linear interpolation from the four closest points (A (57.5°N, 55°E), B (57.5°N, 60°E), C (55°N, 55°E), and D (55°N, 60°E)) was applied to obtain hourly TEC values over Sverdlovsk (Arti) station (56°26'N, 58°34'E)

Given our method and the results of *foF2* and *hmF2* trend extraction (see previous paragraphs), we described the change in TEC for each specific LT moment and each CA index using the following equation:

$$\mathrm{TEC(SP,Y) = c1 + c2(SP) + c3(SP)^2 + c4(SP)^3 + c5(Y - 1994)},$$

where (SP) is the CA index, Y is the year, and c1-c5 are the coefficients of the polynomial. The c5 coefficient is exactly the TEC trend we are looking for. The c1-c5 coefficients were calculated using the least squares method

This method is similar to the method used in the recent work of Urbář and Laštovička [2024] with the only difference: they used a linear dependence on the CA index, whereas we used a polynomial one.

We considered the same three winter months (December, January, and February) the same five LT moments and the same three CA indices (*F30*, *MgII*, and Ly-α) as in our *foF2* trend analysis. The results for the winter months are summarized in Table 8.

Table 8.

Table 8 shows that there is reasonable agreement between the trend values of *k*(TEC) for a particular situation (month, CA index), which is confirmed by the small SD values. The difference between the values of *k*(TEC) for the same month but different CA indices is more significant. At present, we have no explanation for this fact. It is only relevant to note that a similar difference has been obtained in other studies of TEC trends. The values of TEC trends averaged for each month do not differ significantly from each other: the spread is within reasonable limits and allows us to obtain a mean value for winter: -0.126 TECU/year.

To examine seasonal variations in TEC trends, we calculated *k*(TEC) values for April, July, and October. To avoid overloading the paper with large tables, we present in Table 9 the values of *k*(TEC) averaged over the five LT moments.

Table 9.

A brief review of recent publications on the search for TEC trends can be found in Danilov and Berbeneva [2025]. Here we only note that the mean value for winter (-0.126 TECU/yr) is in good agreement with the values of -0.108 TECU/yr and - 0.070 TECU/yr published recently by Urbář and Laštovička [2024] and Elias et al. [2024], respectively.

5. DISCUSSION

The aim of this work was to determine from data of the Sverdlovsk (Arti) station the long-term trends of three parameters of the *F2* layer: the *foF2* critical frequency, the hmF2 height, and the total electron content TEC. Since several researchers have found that *foF2* trends are strongest in winter, we focused our analysis on data from three winter months: December, January, and February. Similarly, because there are diurnal variations in *foF2* trends, we considered five near-midday LT moments.

To remove the effects of solar activity, we used three CA indices (*F30*, *MgII*, and Ly-α), which are considered by many researchers to be the best to describe the variations of the F2 layer with solar activity (see Danilov and Berbeneva [2024]).

A brief review of recent publications on the search for foF2 trends can be found in Danilov and Berbeneva [2025]. We compare here the mean winter trend (-0.034 MHz/year) found for Sverdlovsk station with the results of Danilov et al. [2024б]. For Moscow station, the trend averaged over the same LT moments and CA indices was obtained as -0.025 MHz/year for January and -0.036 MHz/year for February. The same values for Boulder station are -0.028 MHz/yr and -0.033 MHz/yr, respectively, and for Juliusruh station they are -0.035 and -0.041 MHz/yr , respectively. We believe that the agreement between the *k*(*foF2*) values for Sverdlovsk station and the foF2 trends obtained for the three midlatitude stations of the Northern Hemisphere can be considered good.

Comparison of the *foF2* trends for winter with the trends obtained for other months confirmed the existence of seasonal variations of these trends. The amplitudes of the negative *foF2* trends for the summer month of July are significantly smaller than for the winter trends. The trends for the equinox months lie between the winter and summer trends.

In some panels of Figures 1-3, we have marked the behavior of the value of Δ foF2 over several recent months with a dashed line. It can be seen that the slope of this line is stronger (sometimes significantly) than the slope of the main interpolation. This effect is not observed for all situations, so we will not discuss it here. We only note that the problem of possible intensification of *foF2* trends in recent years may be very important. A detailed discussion of this problem based on data for several stations can be found in Danilov et al. [2023b] and Danilov and Berbeneva [2023].

To the same *foF2* values from observations at Sverdlovsk station, we applied the "Delta" method. This method does not allow us to determine the *foF2* trend values themselves, but simply and clearly demonstrates the character of changes in the critical frequency (or height) of the *F2* layer from the earlier period 1958-1980 (which we call "reference") to the later periods 1996-2024 and 2013-2024. It is obtained that the same pattern is observed for all situations - the value of *D*(foF2) is negative and its magnitude is higher for the later period 2013-2024 than for the period 1996-2024. In other words, the values of *foF2* at each fixed CA level are smaller in the analyzed periods than in the reference period 1958-1980. Moreover, this decrease is stronger for the later analyzed period.

The results obtained in this work were in reasonable agreement with the results of determining the *D*(*foF2*) values for Juliusruh station. Thus, it can be stated that, on average, the decrease of *foF2* values when passing from the reference period to the recent decade is about 0.8-0.9 MHz for the data of Sverdlovsk station. Sverdlovsk approximately 0.8-0.9 MHz. This agrees with the negative trends of the critical frequency obtained by the main method

A detailed analysis of *hmF2* trends from data of the Northern and Southern Hemisphere stations was performed by Danilov et al. [2024б]. The same LT moments and the same SA indices for January and February were considered. It was obtained that the mean values of *k*(*hmF2*) for station Moscow are -0.94 and -0.62 km/yr for January and February, respectively. The corresponding values for Juliusruh station are equal to -0.56 and -0.44 km/year.

It can be seen that the *hmF2* trends for Sverdlovsk station are quite close to those for Moscow station, but higher than for Juliusruh station. The mean values of *k*(*hmF2*) are -0.78 km/year for Moscow station and -0.50 km/year for Juliusruh station. Averaging over three winter months gives for Sverdlovsk station the value of -1.05 km/year.

The difference in the values of *k*(*hmF2*) between different stations seems natural, since they are separated by large distances and there are spatial variations in the trends of the *F2* layer parameters (see e.g. Urbář and Laštovička [2024]).

An important feature of our results on *hmF2* trends is the fact that, in contrast to foF2 trends, no significant seasonal variations of *k*(*hmF2*) values were found. The absence of seasonal variations of *hmF2* trends was discussed in Danilov et al. [2024в]. The difference in the seasonal variations of *foF2* and *hmF2* trends indicates, in our opinion, a complex picture of the physical processes leading to these trends.

As in the case of foF2, we applied the Delta method to the *hmF2* data for Sverdlovsk station, used for trend analysis by the main method. We obtained a reasonable agreement of the Delta values for two winter months: for all situations (LT moment, CA index) the same pattern is observed - the *D*(hmF2) values are negative and their magnitude is higher for the later period 2013-2024 than for the period 1996-2024. In other words, the height of the *F2* layer at each fixed CA level is smaller in the analyzed periods than in the reference period 1958-1980. Moreover, this decrease is stronger for the later analyzed period.

Although the Delta method does not give the magnitude of the trend, the results obtained by this method for both foF2 and hmF2 indirectly confirm the negative trends of these parameters obtained by the main method.

Using the global TEC maps, we calculated the trends of the total electron content for the Sverdlovsk (Arti) position. As shown in Subsection 2.3, the results obtained are in good agreement with the results of other recent publications on this topic.

Comparison of trends of different parameters of the F2 layer was considered in Elias et al. [2024] and Danilov and Konstantinova [2024]. Here we will compare the average trends for winter obtained in Section 2.

The mean trends for winter are obtained as -0.034 MHz/yr for *foF2*, -1.05 km/yr for hmF2, and -0.126 TECU/yr for TEC. Since all three trends are measured in different units, we converted them to relative trends in percentages for comparison. If we conditionally assume that the average values of *foF2*, *hmF2* and TEC are 8 MHz, 300 km and 30 TECU, respectively, we obtain that the relative trends of *foF2*, *hmF2* TEC are -0.4%/year, -0.33%/year and -0.4%/year, respectively.

Since TEC is the result of integrating the electron concentration rather than the critical frequency, we doubled the foF2 trend value for comparison (since *NmF2* ~ ($foF2^{)(2)}$) to obtain an NmF2 trend of -0.8% per year. This shows that the relative trend of *NmF2* is slightly higher than the relative trend of TEC. This may be mainly because the upper part of the *F* region may experience weaker decrease due to thermospheric cooling than NmF2. However, this difference is small compared to the scatter of trend values obtained for different situations, so its nature is not worth discussing in detail.

4. CONCLUSION

In this paper, we consider the trends of three parameters of the ionospheric layer *F2*. The critical frequency was measured by the vertical sounding method at Sverdlovsk station (Arti). The *hmF2* values were calculated from the M3000 parameter obtained in the same measurements. To the best of our knowledge, the Sverdlovsk (Arti) station data have never been used to find trends before.

We hope that the results obtained here provide another confirmation of the concept of the existence of significant negative trends of *foF2* and *hmF2* during the last decades due to thermospheric cooling and subsidence [Laštovička et al., 2008]. These results confirm the existence of seasonal variations of *foF2* trends: strong negative trends in winter and relatively weak trends in summer. However, no significant seasonal variations in the trends of F2 layer height *hmF2* were found.

Using the global TEC maps, we calculated the trends of the total electron content above Sverdlovsk station (Arti). The results were in good agreement with the trends obtained in the publications of other authors.

It is obtained that the trends of all three parameters of the F2 layer are negative. This shows that the layer has been decreasing and becoming thinner during the previous decades. The relative trends of *NmF2* and TEC are of the same order of magnitude, with the NmF2 trend magnitude only slightly higher than the TEC trend magnitude.

ACKNOWLEDGEMENTS

TEC data were taken from the global TEC maps on the IZMIRAN website: (https://www.izmiran.ru/ionosphere/weather/grif/Maps/TEC/).

REFERENCES

1. *Danilov A.D., Berbeneva N.A.* Trends of the critical frequency of the *F2* layer in the last decade // Geomagnetism and Aeronomy. T. 63. № 2. C. 139-146. 2023. https://doi.org/10.31857/S0016794022600697

2. *Danilov A.D., Berbeneva N.A.* Dependence of *foF2* on the solar activity indices from data of ionospheric stations of the Northern and Southern Hemispheres // Geomagnetism and Aeronomy. T. 64. № 2. C. 253-264. 2024. https://doi.org/10.31857/S0016794024020083

3. *Danilov A.D., Berbeneva N.A.* Trends of the *F* region parameters and their possible causes // Geomagnetism and Aeronomy. T. 65. № 2. C. 2025.

4. *Danilov A.D., Konstantinova A.V.* Variations of *foF2* trends with season and time of day // Geomagnetism and Aeronomy. T. 55. № 1. C. 56-63. 2015. https://doi.org/10.7868/S0016794015010046

5. *Danilov A.D., Konstantinova A.V.* Long-term changes of the parameter "Delta *foF2*" from data of two European ionospheric stations // Geomagnetism and Aeronomy. T. 57. № 5. C. 623-627. 2017. https://doi.org/10.7868/S0016794017050054

6. *Danilov A.D., Konstantinova A.V.* Comparison of trends of different parameters of the *F2* layer // Geomagnetism and Aeronomy. T. 64. № 5. C.723-724. 2024.

7. *Danilov A.D., Konstantinova A.V., Berbeneva N.A.* Further detailed analysis of *foF2* dependence on solar activity // Heliogeophysical Research. Issue. 40. C. 68-80. 2023a. https://doi.org/10.5425/2304-7380_2023_40_68

8. *Danilov A.D., Konstantinova A.V., Berbeneva N.A.* Detailed analysis of daily variations of *foF2* trends // Heliogeophysical Research. Issue. 39. C. 8-16. 2023б https://doi.org/10.5425/2304-7380_2023_39_8

9. *Danilov A.D., Konstantinova A.V., Berbeneva N.A.* Trends of the critical frequency *foF2* from data of the stations of the Northern and Southern Hemispheres // Geomagnetism and Aeronomy. T. 64. № 3. C. 387-400. 2024a. https://doi.org/10.31857/S0016794024030059

10. *Danilov A.D., Konstantinova A.V., Berbeneva N.A.* Long-term trends of the maximum height of the ionospheric layer *F2* // Geomagnetism and Aeronomy. T. 64. № 4. C. 489-502. 2024б.

11. *Danilov A.D., Konstantinova A.V., Berbeneva N.A.* Variation with time of the ratio between the critical frequency and the *F2* layer height // Geomagnetism and Aeronomy. T. 64. № 5. C. 656-666. 2024в.

12. *Cnossen I., Emmert J.T. Garcia R.R., Elias A.G., Mlynczak M.G., Zhang Sh.R..* A review of global long-term changes in the mesosphere, thermosphere and ionosphere: a starting point for inclusion in (semi-)empirical models // Adv. Space Res. V. 74. N 11. P. 5991-6011. 2024. https://doi.org/10.1016/j.asr.2024.10.005

13. *Danilov A.D., Berbeneva N.A.* Statistical analysis of the critical frequency *foF2* dependence on various solar activity indices // Adv. Space Res. V. 72. N 6. P. 2351-2361. 2023. https://doi.org/10.1016/j.asr.2023.05.012

14. *De Haro Barbás B. F., Elias A. G.* Effect of the inclusion of solar cycle 24 in the calculation of *foF2* long-term trend for two Japanese ionospheric stations // Pure Appl. Geophys. V. 177. N 2. P. 1071-1078. 2020. https://doi.org/10.1007/s00024-019-02307-z

15. *De Haro Barbás D.F., Elias A.G., Venchiarutti J.V., Fagre M., Zossi B.S., Jun G.T., Medina F.D.* MgII as a solar proxy to filter *F2-region* ionospheric parameters // Pure Appl. Geophys. V. 178. N 11. P. 4605-4618. 2021. https://doi.org/10.1007/s00024-021-02884-y

16. *Duran T. Melendi Y., Zossi B.S., de Haro Barbás B.F., Buezas F.S., Alfredo Juan A., Elias A.G.* Contribution to ionospheric *F2* region long-term trend studies through seasonal and

diurnal pattern analysis // Global Planet. Change. V. 229. ID 104249. 2023. https://doi.org/10.1016/j.gloplacha.2023.104249

17. *Elias A. Alberti T., Bravo M. et al.* Long-term trends in the ionospheric equivalent slab thickness: Some evidences by Working Team #1 within IAGA WGII-F // Paper presented at the 12th International Workshop on Long-Term Changes and Trends in the Atmosphere. May 6-10, 2024. Ourense, Galicia, Spain. 2024.

18. *Laštovička J., Akmaev R.A., Beig G., Bremer J., Emmert J.T., Jacobi C., Jarvis M.J., Nedoluha G., Portnyagin Yu.I., Ulich T.* Emerging pattern of global change in the upper atmosphere and ionosphere // Ann. Geophys. V. 26. N 5. P. 1255-1268. 2008. https://doi.org/10.5194/angeo–26–1255–2008

19. *Laštovička J.* Progress in investigating long-term trends in the mesosphere, thermosphere, and ionosphere // Atmos. Chem. Phys. V. 23. N 10. P. 5783-5800. 2023. https://doi.org/10.5194/acp-23-5783-2023

20. *Laštovička J.* Dependence of long-term trends in *foF2* at middle latitudes on different solar activity proxies // Adv. Space Res. V. 73. N 1. P. 685– 689. 2024. https://doi.org/10.1016/j.asr.2023.09.047

21. *Laštovička J., Burešová D.* Relationships between *foF2* and various solar activity proxies // Space Weather. V. 21. N 4. ID e2022SW003359. 2023. https://doi.org/10.1029/2022SW003359

22. *Urbář J., Laštovička J.* Global long-term trends in the total electron content // Preprint EGUsphere. ID 3021. 9 p. 2024. https://doi.org/10.5194/egusphere-2024-3021

23. *Yue X., Hu L., Wei Y., Wan W., Ning B*. Ionospheric trend over Wuhan during 1947-2017: Comparison between simulation and observation // J. Geophys. Geophys. Res. - Space. V. 123. N 2. P. 1396-1409. 2018. https://doi.org/10.1002/2017JA024675

24. *Zossi B.S., Medina F.D., Duran T., Elias A.G.* The effect of mixing EUV proxies on the correlation with *foF2* and on long-term trends estimates // Adv. Space Res. V. 74. N. 10. P. 4930-4936. 2024. https://doi.org/10.1016/j.asr.2024.07.064

25. *Zossi B.S., Medina F.D., Duran T., Elias A.G.* Selecting the best solar EUV proxy for long-term timescale applications // Adv. Space Res. V.75. N 1. P. 856-863. 2025. https://doi.org/10.1016/j.asr.2024.07.023

Table 1: *foF2* trends in MHz/year for three winter months

Month	Local time	CA index					
		F30		Ly-α		MgII	
		trend, MHz/year	R^2	trend, MHz/year	R^2	trend, MHz/year	R^2
December	10 LT	-0.021	0.38	-0.016	0.54	-0.032	0.77
	11 LT.	-0.036	0.71	-0.038	0.84	-0.040	0.94
	12 LT.	-0.030	0.70	-0.023	0.81	-0.045	0.91
	13 LT.	-0.040	0.79	-0.036	0.83	-0.034	0.83
	14 LT	-0.029	0.80	-0.020	0.80	-0.035	0.87
	Average for 10-14 LT	-0.031	-	-0.026	–	-0.037	–
	SD	0.007	-	0.009	–	0.005	-
January	10 LT	-0.038	0.86	-0.033	0.80	-0.031	0.92
	11 LT.	-0.037	0.81	-0.036	0.82	-0.041	0.92
	12 LT.	-0.039	0.78	-0.034	0.87	-0.043	0.94
	13 LT.	-0.036	0.76	-0.027	0.79	-0.037	0.94
	14 LT	-0.045	0.84	-0.032	0.85	-0.049	0.97
	Average for 10-14	-0.040	–	-0.032	-	-0.040	–
	SD	0.005	-	0.003	–	0.007	-
February	10 LT	-0.035	0.90	-0.033	0.83	-0.042	0.88
	11 LT.	-0.028	0.87	-0.031	0.72	-0.035	0.77
	12 LT.	-0.028	0.79	-0.034	0.70	-0.035	0.74
	13 LT.	-0.037	0.88	-0.033	0.74	-0.043	0.79
	14 LT	-0.032	0.88	-0.032	0.75	-0.038	0.79
	Average for 10-14 LT	-0.032	-	-0.033	-	-0.039	-
	SD	0.004	-	0.001	-	0.004	-

Table 2. *D*(*foF2*) values in MHz for January and February.

CA index	Local time	January		February	
		1996-2024	2013-2024	1996-2024	2013-2024
F30	10 LT	-0.39	-0.74	-0.69	-0.83
	11 LT.	-0.48	-0.94	-0.65	-0.75
	12 LT.	-0.59	-0.95	-0.67	-0.80
	13 LT.	-0.64	-0.97	-0.69	-0.92
	14 LT	-0.39	-0.68	-0.63	-0.78
	LT average	-0.50	-0.86	-0.65	-0.82
	SD	0.11	0.14	0.03	0.07
Ly-α	10 LT	-0.73	-0.83	-0.92	-1.03
	11 LT.	-0.91	-1.05	-0.93	-0.99
	12 LT.	-0.90	-1.07	-0.96	-1.04
	13 LT.	-0.95	*-1.09*	-0.99	-1.16
	14 LT	-0.42	-0.62	-0.93	-1.07
	LT average	-0.78	-0.93	-0.95	-1.06
	SD	0.21	0.20	0.03	0.06
MgII	10 LT	-0.45	-0.63	-0.76	-0.88
	11 LT.	-0.58	-0.86	-0.76	-0.85
	12 LT.	-0.59	-0.88	-0.80	-0.97
	13 LT.	-0.60	0.90	-0.77	0.99
	14 LT	-0.30	-0.58	-0.69	-0.88
	LT average	-0.50	-0.77	-0.76	-0.91
	SD	0.13	0.15	0.04	0.06
	Average of *F30*, *Ly*,	-0.59	-0.85	-0.79	-0.93

Table 3: Comparison of *D*(*foF2*) values in MHz for the two stations.

Month	Station					
	Sverdlovsk			Juliusruh		
	Years	Ly-α	MgII	Years	Ly-α	MgII
January	1996-2024	-0.78	-0.50	1996-2022	-0.88	-0.53

	2013-2024	-0.93	-0.77	2013-2022	-0.92	-0.71
February	1996-2024	-0.95	-0.76	1996-2022	-0.73	-0.61
	2013-2024	-1.06	-0.91	2013-2022	-0.91	-0.60

Table 4. Trend values of *foF2* in MHz/year for April, July and October

Month	F30		MgII		Ly-α		Average by 3 indices
	k(*foF2*)	SD	*k*(*foF2*)	SD	*k*(*foF2*)	SD	
April	−0.022	0.008	−0.029	0.009	−0.019	0.011	−0.023
July	−0.010	0.004	−0.016	0.002	−0.013	0.003	−0.013
October	−0.018	0.002	−0.024	0.004	−0.018	0.002	−0.020

Table 5: Trends of *hmF2* in km/year for winter months

Local time	CA index						month
	F30		Ly-α		MgII		January
	trend	R^2	trend	R^2	trend	R^2	
10 LT	-1.40	0.83	-1.30	0.85	-1.20	0.79	
11 LT.	-1.49	0.86	-1.40	0.90	-1.33	0.92	
12 LT.	-1.19	0.95	-1.11	0.96	-1.31	0.97	
13 LT.	-0.93	0.84	-1.07	0.90	-1.09	0.93	
14 LT	-1.02	0.92	-1.07	0.96	-1.15	0.96	
LT average	-1.21		-1.19		-1.22		
SD	0.24		0.15		0.10		
Average of 3 indices	-1.21						
10 LT	-0.92	0.89	-0.72	0.84	-1.01	0.95	February
11 LT.	-0.78	0.75	-0.77	0.82	-0.88	0.85	
12 LT.	-0.84	0.84	-0.62	0.91	-1.03	0.91	
13 LT.	-0.98	0.96	-0.73	0.96	-0.94	0.94	
14 LT	-0.79	0.78	-0.56	0.83	-0.88	0.90	
LT average	-0.86		-0.68		-0.95		
SD	0.09		0.09		0.07		
Average of 3 indices	-0.83						

Table 6: Trend values of *hmF2* in km/year for four months

Month	F30		MgII		Ly-α		Average of 3 indices
	k(*hmF2*)	SD	*k*(*hmF2*)	SD	*k*(*hmF2*)	SD	
April	−0.64	0.10	−0.80	0.12	−0.83	0.08	−0.76
June	−0.90	0.21	−1.00	0.14	−1.08	0.22	−0.99
July	−0.80	0.10	−0.82	0.09	−0.85	0.07	−0.82
October	−0.94	0.14	−0.81	0.16	−0.93	0.19	−0.79

Table 7. Values of *D*(*hmF2*) in km for January and February

CA index	Local time	January		February	
		1996-2024	2013-2024	1996-2024	2013-2024
F30	10 LT	-13.4	-21.6	-14.2	-20.5
	11 LT.	-17.2	-28.2	-14.4	-18.6
	12 LT.	-15.0	-23.6	-15.1	-17.4
	13 LT.	-13.9	-20.7	-20.4	-22.6
	14 LT	-16.2	-23.3	-17.3	-18.0
	LT average	-15.1	-23.5	-16.3	-19.4
	SD	1.6	2.9	3.6	2.1
Ly-α	10 LT	-16.6	-23.1	-15.0	-21.0
	11 LT.	-18.2	-30.0	-15.2	-20.8
	12 LT.	-16.2	-25.0	-15.6	-18.6
	13 LT.	-13.8	-20.8	-21.8	-23.6
	14 LT	-17.9	-25.0	-18.2	-20.3
	LT average	-16.0	-24.8	-17.2	-20.9
	SD	1.7	3.4	2.9	1.8
MgII	10 LT	-14.6	-21.2	-13.6	-20.4
	11 LT.	-15.7	-27.8	-13.5	-18.9
	12 LT.	-14.4	-22.8	-14.1	-17.0
	13 LT.	-12.0	-18.5	-18.4	-22.6

	14 LT	-14.3	-21.8	-16.5	-18.7
	LT average	-14.2	-22.4	-15.2	-19.5
	SD	1.4	3.4	2.2	2.1
	Average of 3 indices	-15.3	-23.6	-16.2	-19.9

Table 8: TEC trends in TECU/year for winter months

local time	CA index			month
	F30	MgII	Ly-α	
10 LT	-0.076	-0.101	-0.111	January
11 LT.	-0.091	-0.125	-0.137	
12 LT.	-0.114	-0.151	-0.165	
13 LT.	-0.121	-0.151	-0.166	
14 LT	-0.093	-0.131	-0.144	
LT average	-0.099	-0.132	-0.145	
SD	0.018	0.021	0.023	
Average of 3 indices	-0.123			
10 LT	-0.121	-0.102	-0.119	February
11 LT.	-0.149	-0.125	-0.148	
12 LT.	-0.152	-0.127	-0.151	
13 LT.	-0.160	-0.134	-0.159	
14 LT	-0.153	-0.127	-0.151	
LT average	-0.147	-0.123	-0.146	
SD	0.015	0.012	0.015	
Average of 3 indices	-0.139			
10 LT	-0.074	-0.122	-0.153	December
11 LT.	-0.072	-0.133	-0.172	
12 LT	-0.078	-0.144	-0.187	
13 LT.	-0.040	-0.108	-0.152	
14 LT	-0.051	-0.113	-0.154	
LT average	-0.063	-0.124	-0.164	
SD	0.017	0.015	0.015	
Average of 3 indices	-0.117			

Table 9. TEC trend values in TECU/year for three months

month	F30		MgII		Ly-α		Average 3 indices
	k(TEC)	SD	*k*(TEC)	SD	*k*(TEC)	SD	
April	-0.098	0.010	-0.181	0.011	-0.194	0.012	-0.158

July	-0.081	0.007	-0.106	0.009	-0.092	0.007	-0.093
October	-0.035	0.009	-0.102	0.014	-0.120	0.015	-0.086

FIGURE CAPTIONS

Figure 1. Examples of changes in Δ *foF2* with time for December.

Figure 2. Examples of changes in Δ *foF2* with time for January.

Figure 3. Examples of changes in Δ *foF2* with time for February.

Figure 4. Dependencies of *foF2* on CA indices for different years in January.

Figure 5. Dependencies of *foF2* on CA indices for different years in February.

Figure 6. Examples of change in Δ *foF2* with time for April and October.

Figure 7. Examples of *ΔhmF2* variation with time for December.

Figure 8. Examples of *ΔhmF2* variation with time for January.

Figure 9. Examples of *ΔhmF2* variation with time for February.

Figure 10. Examples of change in *ΔhmF2* with time for four months.

Figure 11. Examples of *ΔhmF2* variation with time for different time periods intervals in January and February.

Figure 1.

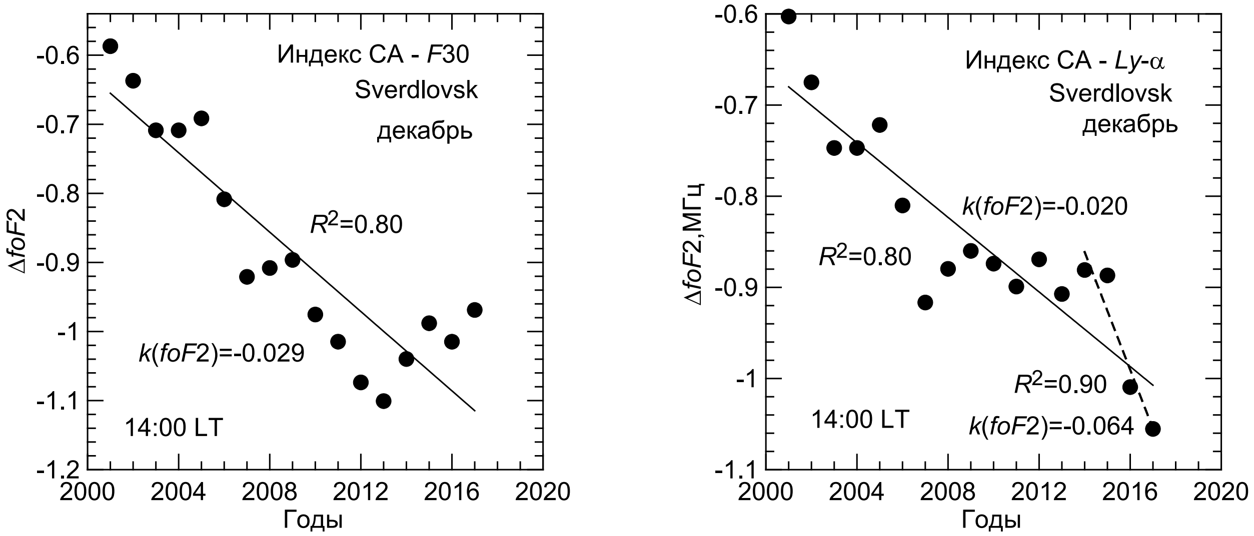

Figure 2

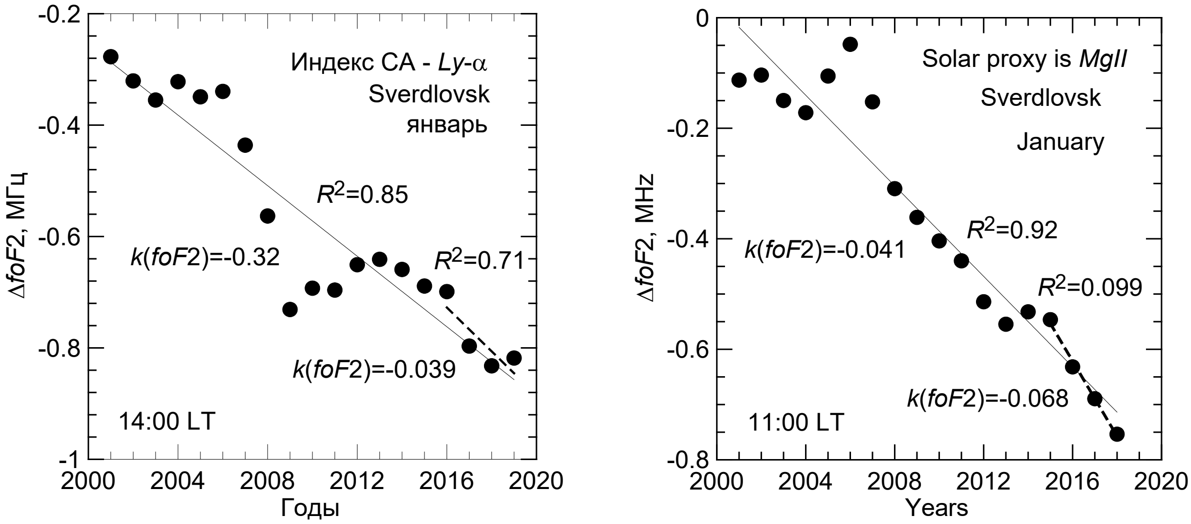

Figure 3

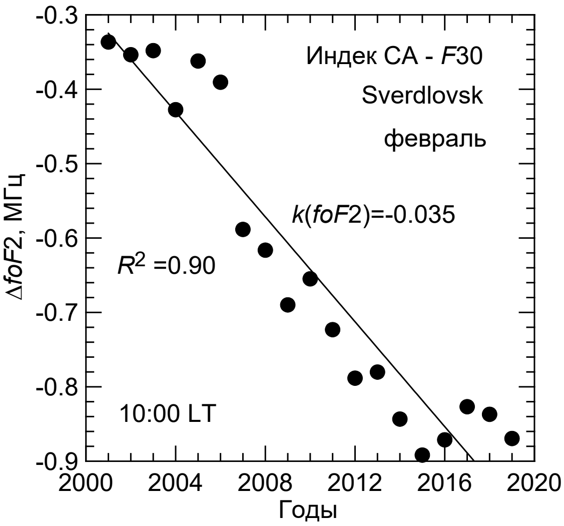

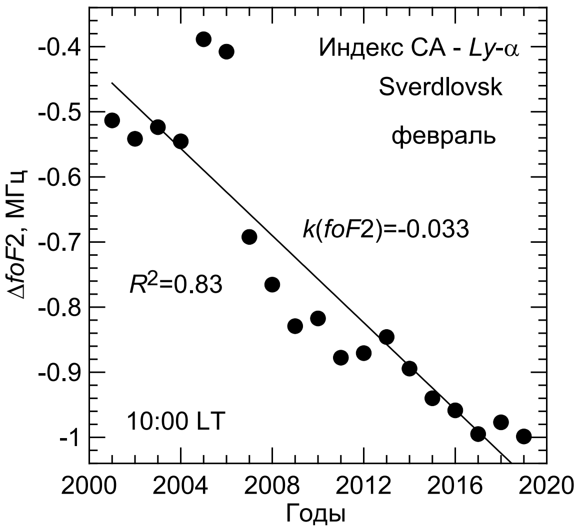

Figure 4

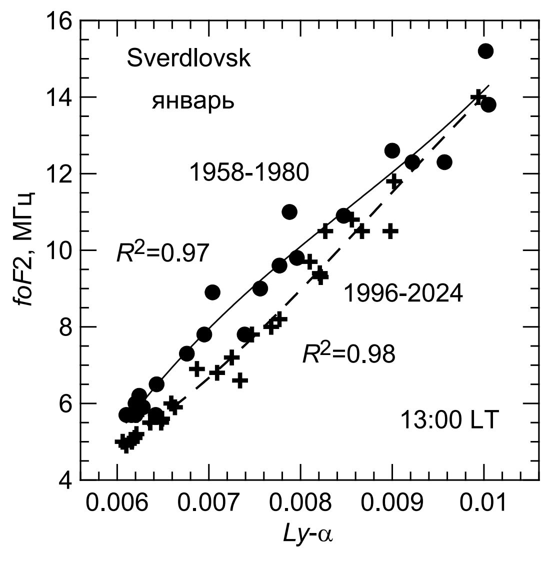

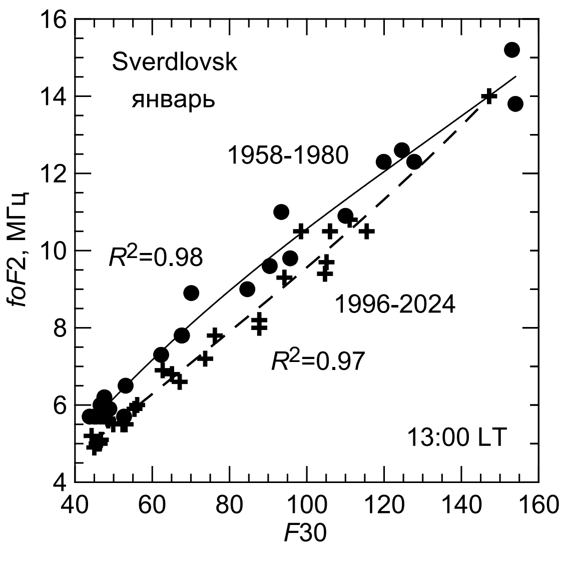

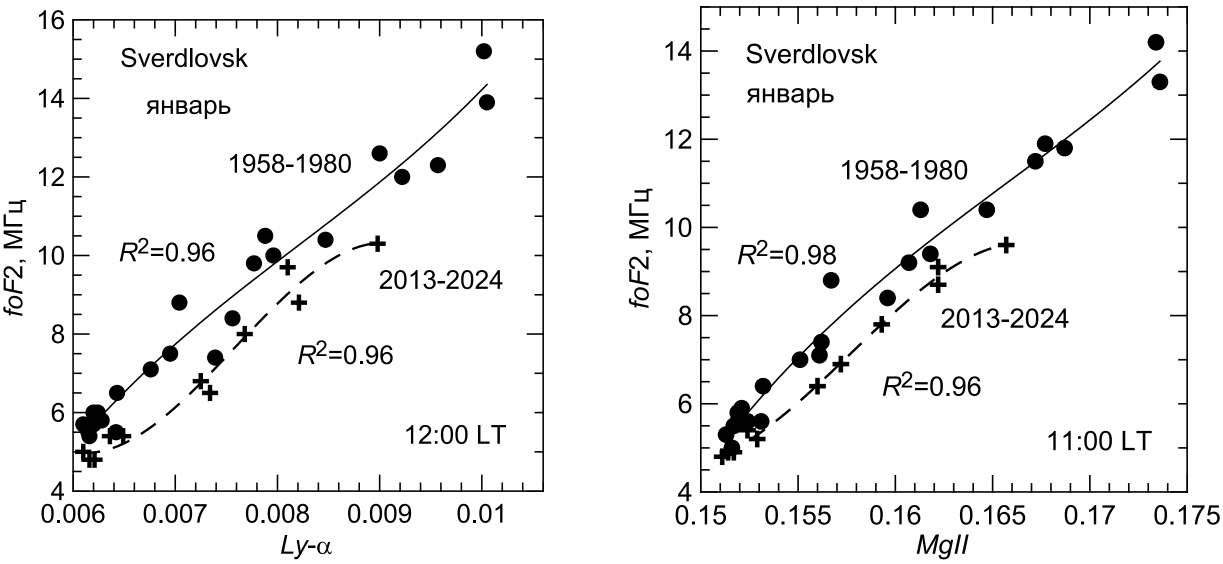
Sverdlovsk
январь
1958-1980
R2=0.96
2013-2024
R2=0.96
12:00 LT
foF2, МГц
Ly-α
Sverdlovsk
январь
1958-1980
R2=0.98
2013-2024
R2=0.96
11:00 LT
foF2, МГц
MgII

Figure 5.

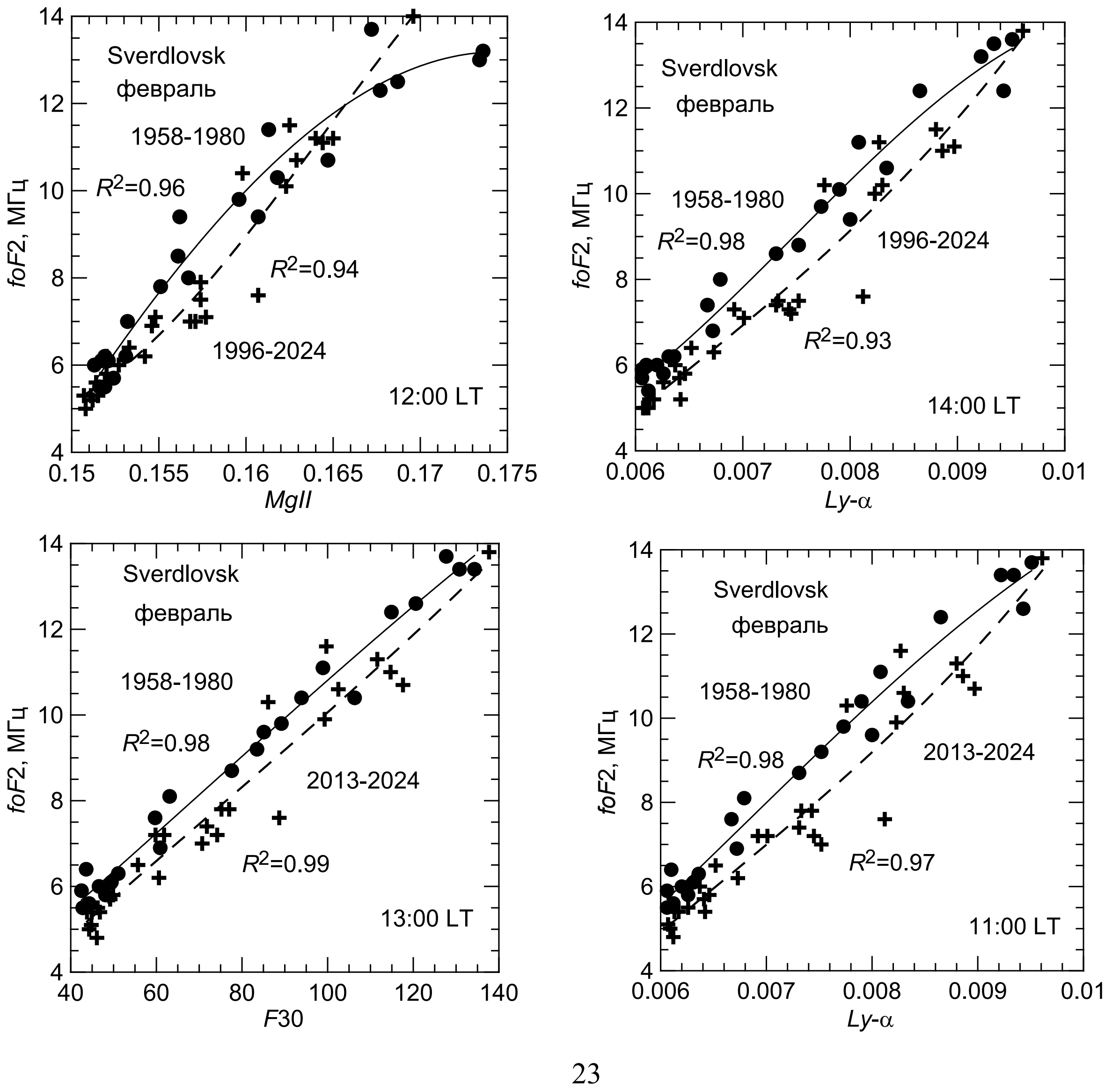
Sverdlovsk
февраль
1958-1980
R2=0.96
R2=0.94
1996-2024
12:00 LT
foF2, МГц
MgII
Sverdlovsk
февраль
1958-1980
R2=0.98
1996-2024
R2=0.93
14:00 LT
foF2, МГц
Ly-α
Sverdlovsk
февраль
1958-1980
R2=0.98
2013-2024
R2=0.99
13:00 LT
foF2, МГц
F30
Sverdlovsk
февраль
1958-1980
R2=0.98
2013-2024
R2=0.97
11:00 LT
foF2, МГц
Ly-α

Figure 6

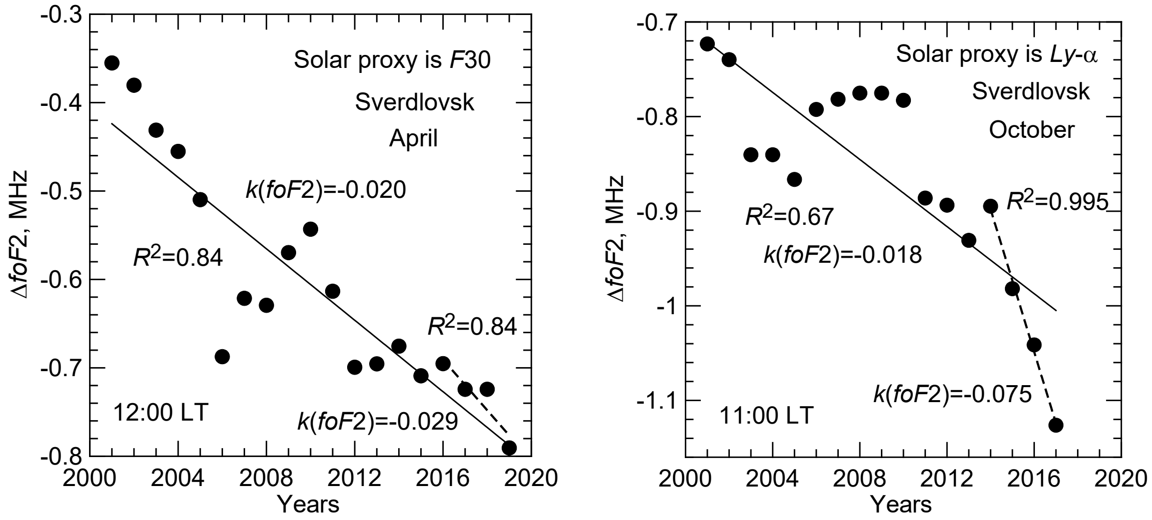

Figure 7

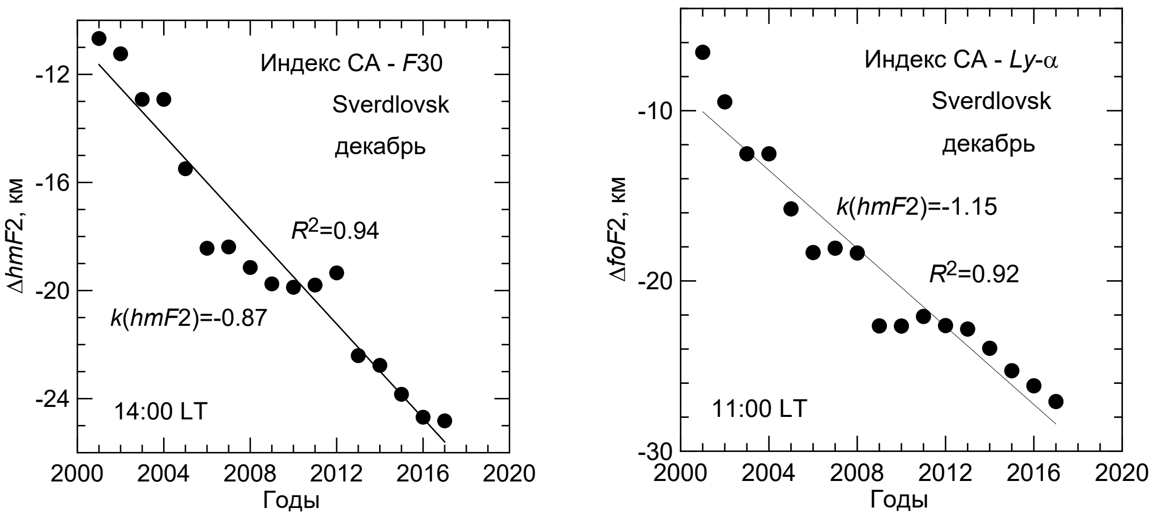

Figure 8.

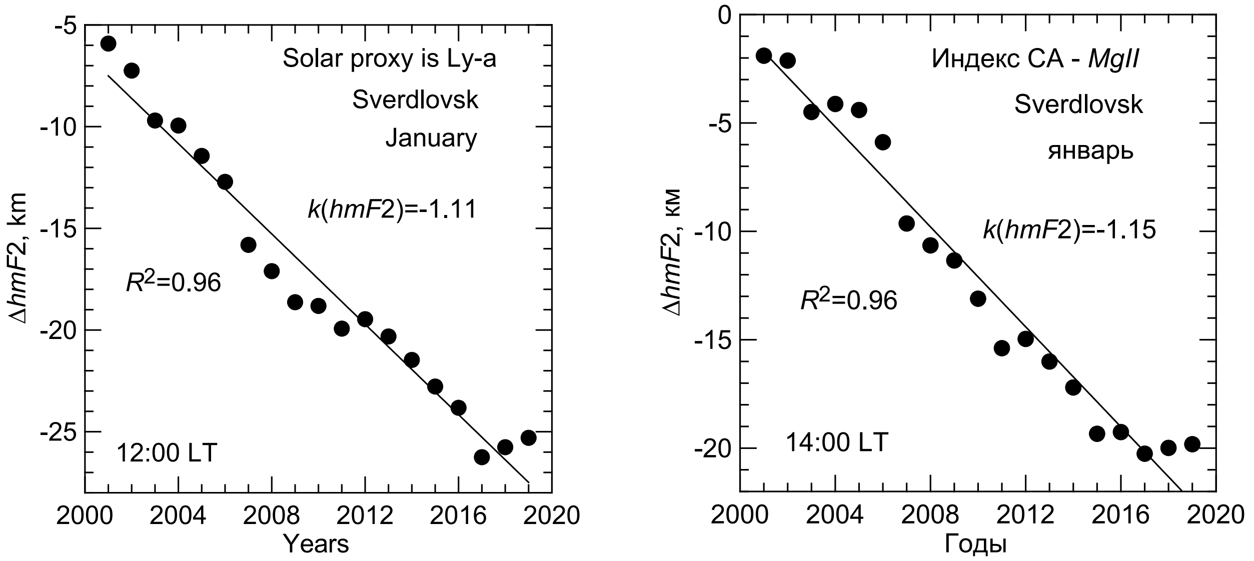

Figure 9.

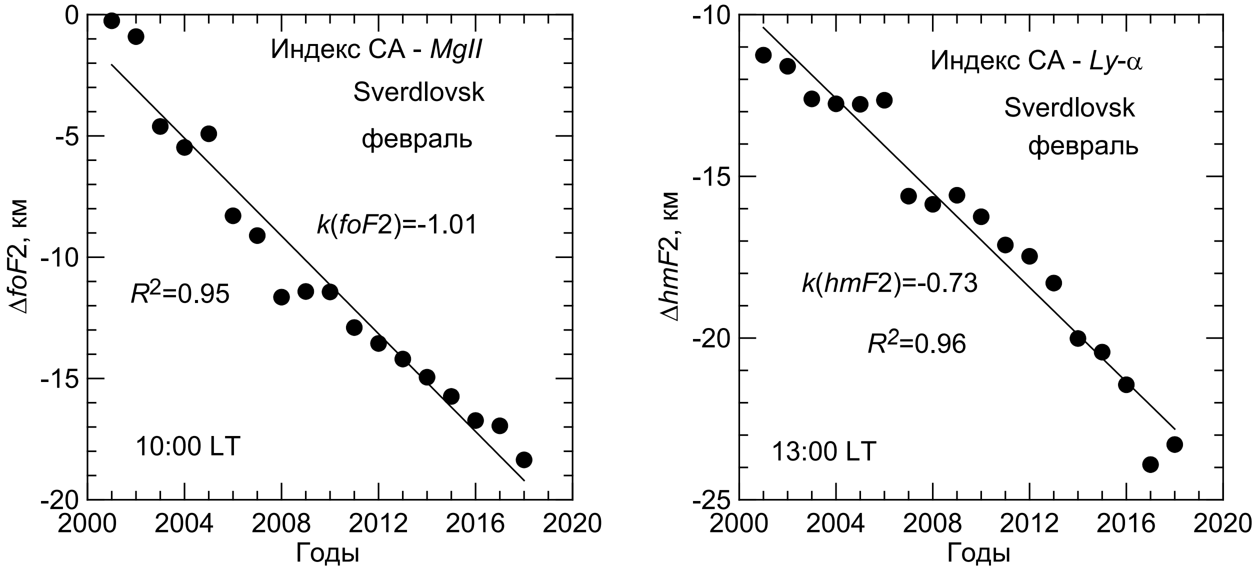

Figure 10

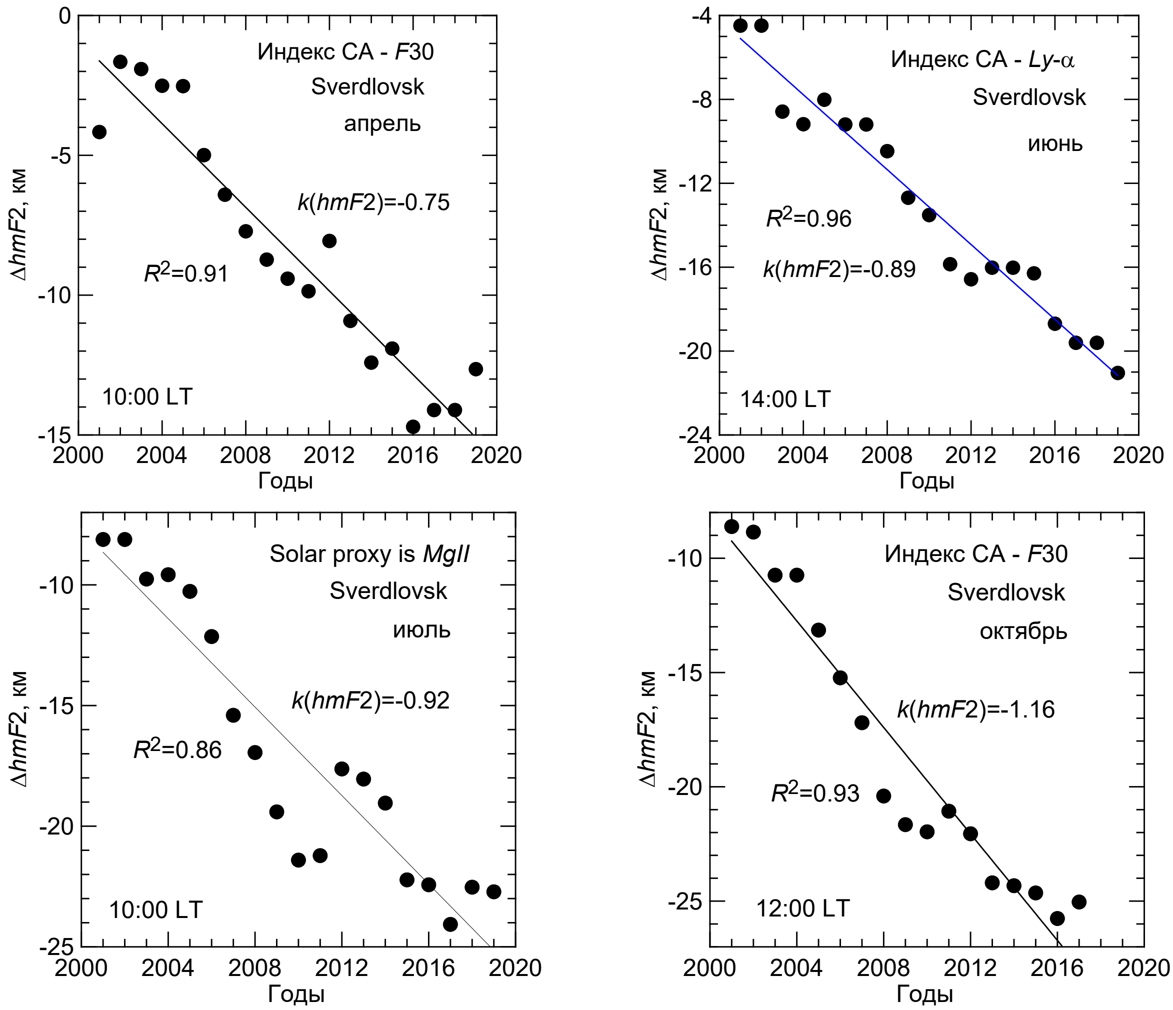

Индекс СА - F30
Sverdlovsk
апрель
k(hmF2)=-0.75
R2=0.91
10:00 LT
ΔhmF2, км
Годы
Индекс СА - Ly-α
Sverdlovsk
июнь
R2=0.96
k(hmF2)=-0.89
14:00 LT
ΔhmF2, км
Годы
Solar proxy is MgII
Sverdlovsk
июль
k(hmF2)=-0.92
R2=0.86
10:00 LT
ΔhmF2, км
Годы
Индекс СА - F30
Sverdlovsk
октябрь
k(hmF2)=-1.16
R2=0.93
12:00 LT
ΔhmF2, км
Годы

Figure 11

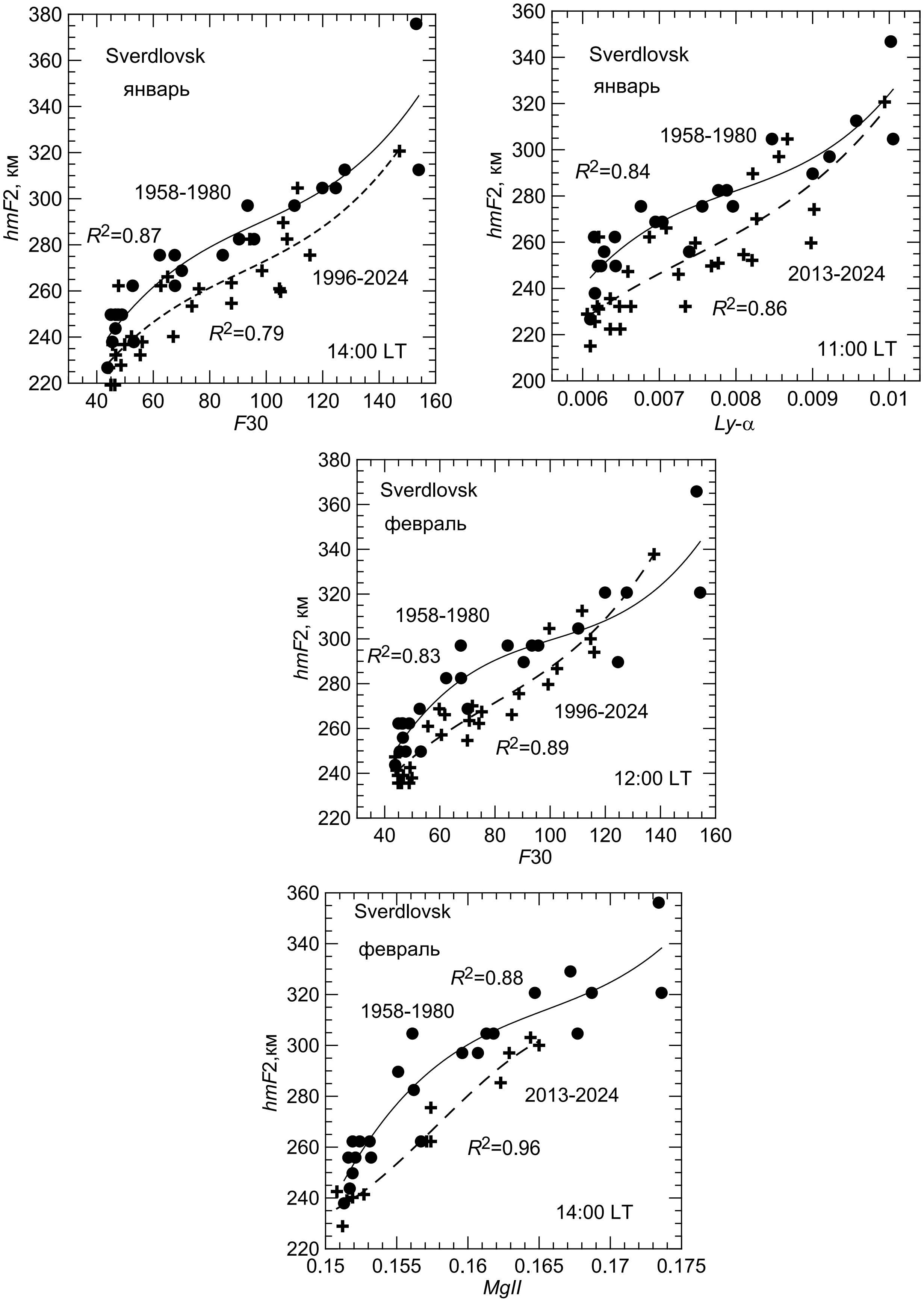
Sverdlovsk
январь
1958-1980
R2=0.87
1996-2024
R2=0.79
14:00 LT
hmF2, км
F30
Sverdlovsk
январь
1958-1980
R2=0.84
2013-2024
R2=0.86
11:00 LT
hmF2, км
Ly-α
Sverdlovsk
февраль
1958-1980
R2=0.83
1996-2024
R2=0.89
12:00 LT
hmF2, км
F30
Sverdlovsk
февраль
R2=0.88
1958-1980
2013-2024
R2=0.96
14:00 LT
hmF2,км
MgII